Hydrated Structure of Ag(I) Ion from Symmetry-Dependent, K- and L-Edge XAFS Multiple Scattering and Molecular Dynamics Simulations

John L. Fulton,*,† Shawn M. Kathmann,† Gregory K. Schenter,† and Mahalingam Balasubramanian‡

Chemical and Materials Sciences Division, Pacific Northwest National Laboratory, Richland, Washington 99354, and Advanced Photon Source, Argonne National Laboratory, Argonne, Illinois 60439

Received: July 9, 2009; Revised Manuscript Received: September 4, 2009

Details of the first-shell water structure about Ag^+ are reported from a corefinement of the K- and L_2-edge multiple scattering signal in the X-ray absorption fine structure (XAFS) spectra. Detailed fits of the Ag K-edge data that include the contributions from multiple scattering processes in the hydrated ion structure cannot distinguish between models containing tetrahedral symmetry versus those containing collinear O−Ag−O bonds. However, we show that the multiple scattering oscillations at the L_2-edges have distinctly different phase and amplitude functions than at the K-edge. These phase and amplitude functions depend not only on the symmetry of the multiple scattering paths but also on the nature of the final state electronic wave function probed by the dipole-allowed transition. Hence the multiple scattering portions of K- and L_2-edge spectra provide *independent* measurements of the local symmetry—not a redundant measurement as is commonly believed. On the basis of the enhanced information content obtained by the simultaneous assessment of both the K- and L_2-edges, we report that the hydrated Ag^+ structure contains five or six water molecules in the first shell with a significant number of nearly collinear and 90° O−Ag−O bond angles. Finally, the K- and L_2-edge spectra are used to benchmark the hydration structure that is generated from both DFT-based and classical molecular dynamics simulations. Simulated first-shell structures are compared to the experimental structures.

1. Introduction

A complete understanding of the hydrated structure of cations in aqueous solutions is an essential starting point for understanding their chemistry and dynamics. The Ag^+ cation is not only important in areas of geochemistry, crystallization, and photochemistry, but it is also an interesting analog for understanding the solvation of monovalent cations Na^+ and K^+, since it has an ionic radius that lies between those of Na^+ and K^+ (Ag^+ 1.15 Å, Na^+, 1.02 Å, K^+ 1.38 Å). The study of this heavy metal ion is also a starting point for understanding the chemistry of other second and third row transition elements and ultimately the lanthanides and actinides. The Ag^+ ion has a ground state configuration $[Kr]4d^{10}5s^1$ that frequently undergoes hybridization of $4d_{z^2}$ with 5s orbital, leading to a strong tendency to form 2-fold coordination structures in a linear geometry. Experimental and theoretical studies of gas-phase $Ag^+(H_2O)_n$ clusters generally confirm this tendency of water to form linear structures. For instance, ab initio calculations of small $Ag^+(H_2O)_{2-6}$ clusters[1,2] show a tendency to form collinear O−Ag−O structures for all cluster sizes. In addition, three-coordinate species are also common entities in which the bond angle for two of the three water molecules is about 85°. This study also showed that the lowest energy $Ag^+(H_2O)_6$ cluster has two nearly collinear waters (Ag−O, 2.225 Å; O−Ag−O, 172.6°), two waters in the equatorial plane with a bond angle of approximately 80°, and the remaining two waters residing in the second shell.[1] The experimental values of incremental enthalpies for $Ag^+(H_2O)_{1-6}$ clusters show that the first two water ligands are strongly bound. The binding energy is greatly reduced for the remaining four H_2O,[3] again suggestive of preferential binding for the coaxial water ligands.

Quite in contrast to these gas-phase water cluster studies, earlier aqueous solution studies by diffraction[4−6] and XAFS[7,8] show the silver binding four H_2O in a regular tetrahedral geometry. Recent XAFS and large-angle X-ray scattering studies by Persson[9] suggest a linearly distorted tetrahedral model with two short and two long Ag−O bond distances. This was the first experimental result for a bulk aqueous system that brought into question the accepted view of a regular tetrahedral symmetry for Ag^+.

Molecular simulations of aqueous hydration of Ag^+ present a mixed picture. DFT-based molecular dynamics simulations[10,11] show binding of four or five water molecules, whereas QM/MM molecular dynamics[12] show both 5- and 6-coordinate species in a 2 + 3 and 2 + 4 configuration with two closer water molecules and the remaining waters at longer distances. This simulation result also showed a dominant O−Ag−O bond angle at about 87° and a secondary bond angle at about 160°.

In this report, we analyze the symmetry-dependent multiple scattering of *both* K- and L_2-edge X-ray absorption fine structure (XAFS) spectra to provide key insights into the symmetry of the first hydration shell. Certain multiple scattering paths are only weakly allowed at the K- or L_1-edge (s-electrons) but fully allowed for the L_2- or L_3-edges (2p-electrons). In addition, different multiple scattering geometries lead to different sets of scattering phase shifts for the K- versus the L_2-edges. This is in contrast to the common expectation that the photoelectronic waves for K- or L_1- versus L_2- or L_3-edge XAFS only give rise

* To whom correspondence should be addressed. E-mail: john.fulton@pnl.gov.
† Pacific Northwest National Laboratory.
‡ Argonne National Laboratory.

10.1021/jp9064906 CCC: $40.75
Published on Web 10/19/2009

to a simple π shift factor and thus represent redundant measurements of their structure. These scattering characteristics mean that two completely *independent* measurements of the first shell symmetry are available by measuring both the K- and L_2-edge multiple scattering spectra. This method, although not widely recognized, was pointed out early on by Kuzmin[13,14] and Di Ciccio.[15] A further benefit of measurement at the L_2- or L_3-edge is that the multiple scattering signal is over two times more intense because of the much lower core hole lifetime broadening that attenuates the multiple scattering at the K- or L_1-edges (lifetime broadening is 6.75, 4.88, 2.57, and 2.40 eV for the K-, L_1-, L_2-, and L_3 edges, respectively).[16]

This method of symmetry-dependent, multiedge, multiple scattering analysis is applied to the study of Ag^+ hydration structure. To our knowledge, this approach has not been previously used for study of aqueous solvation. This multiedge analysis is especially suited to hydrated aqueous ions, where the XAFS signal is primarily derived from the first shell structure. The second and higher solvation shells are too disordered to contribute to the signal, thus limiting the overlap of L_3- and L_2-edge XAFS signals into the signal from the next higher edge. The K-edge spectrum, because of it is extended energy range,[17] provides the best opportunity to resolve the Ag−O bond distance and bond disorder, whereas multiple scattering analysis of the K-, L_2-, or L_3-edges provides information about the first-shell symmetry. The Ag L-edges are at relatively low energies, where X-ray transmission through the sample is a limitation. Hence, we used low-energy XAFS methods that we have previously developed for studying the hydration of Cl^-, K^+, and Ca^{2+}.[18−20] We show that corefined fits of the K- and L_2-edge spectra suggest a hydrated Ag^+ with approximately five or six H_2O's in the first shell wherein the symmetry includes a significant number of collinear and 90° O−Ag−O bonds. These results are in excellent agreement with recent simulation structures and are more in line with gas-phase cluster results.

A final objective of this report is to use both K- and L_2-edge spectra to directly benchmark the structure from molecular dynamics simulations. The method of molecular dynamics XAFS (MD-XAFS) uses the ab initio XAFS scattering code to generate a spectrum from a large ensemble of MD snapshots.[19−21] The recent generation of density functional theory based molecular dynamics (DFT-MD) provides significant advantages over simulations using classical potentials by providing for site-specific binding of water to the valence orbitals of the Ag ion. Our interest is to evaluate the quality of both DFT-based and classical MD simulations structure by comparison to the experimental K- and L_2-edge spectra.

2. Experiment and Theory Section

2.1. Chemicals and Procedures. Silver perchlorate monohydrate (99.999%), silver nitrate (99.9999%), and perchloric acid (99.999%) were used as received from Aldrich. Part of the analysis involved studies of well-characterized reference compounds, including Ag_2O (99.99%) and silver chloride (99.998%), that were also used as received from Aldrich. Distilled, deionized water was used throughout. We briefly explored the effects of concentration and pH on the hydrated structure of Ag^+. Spectra from 0.02 and 0.2 *m* $AgClO_4$ and 0.06 *m* $AgNO_3$ were identical, including the multiple scattering feature at about 3.5 Å (see the Supporting Information). This demonstrated that, in the concentration range of this study, there is no tendency to form ion-paired species.[22] Ag^+ undergoes almost no hydrolysis in aqueous solution[23] and samples acidified with 0.002 *m* $HClO_4$ were identical to those without (see the Supporting Information).

2.2. XAFS Experimental Methods. The silver K-edge (25514 eV) and L_2-edge (3524 eV) XAFS spectra were collected in transmission mode on the bending magnet beamline (PNC-CAT, Sector 20) at the Advanced Photon Source, Argonne National Laboratory. At the bending magnet beamline, the photon fluxes at the K- and L-edges are approximately 1×10^9 and 5×10^8 photons/s, respectively. Details of the XAFS beamline methods are given elsewhere.[18,24] At the silver K-edge (25514 eV), the instrumental resolution was estimated to be about 4 eV based upon a slit height of 400 μm. This is somewhat smaller than the core hole lifetime broadening at this edge of 6.75 eV.[25] For the L_2-edge spectra, the X-ray optics and sample holder were similar to what has been previously used.[18,20] The L_2-edge spectra were acquired in transmission mode using pathlengths of 125 or 250 μm.

The fits to the K-edge XAFS $\chi(k)$ data were weighted by k^3 and windowed between $2.0\ \text{Å}^{-1} < k < 13.0\ \text{Å}^{-1}$ using a Hanning window with $dk = 1.0\ \text{Å}^{-1}$. The L_2-edge XAFS $\chi(k)$ data were weighted by k^2 and windowed between $2.0\ \text{Å}^{-1} < k < 7.5\ \text{Å}^{-1}$. The fits were to both the real and imaginary parts of $\tilde{\chi}(R)$ in the region of 1.0 Å $< R <$ 5.0 Å. We used portions of the Athena and Artemis programs for the analysis of XAFS data[26,27] with theoretical standards calculated using FEFF8.[28,29] Three silver-containing standard compounds, silver(I) oxide, silver nitrate, and silver chloride, were used to establish the value of the K-edge core hole factor, $S_0^2 = 0.83$. S_0^2 has an associated uncertainty of about 15% that results in an approximate 15% uncertainty in the reported coordination number. Water coordination numbers where derived from the K-edge spectra, whereas all other structural parameters were derived from corefinement of both the K- and L_2-edge spectra.

The atomic background function, $\mu(E)$, of the K-edge spectra contains significant multielectron excitations that appear in the $\chi(k)$ data at $k = 1.7$, 4.1, 5.4, 10.3, 12.7 Å^{-1}. The later two edges at high k significantly distort the primary Ag−O single scattering signal and thus significantly increase the uncertainty in the measured R, σ^2, and C_3. These multielectron excitations were removed from the background function via measurement of three well-characterized crystalline standards using the procedure described in the Supporting Information. This approach avoids the use of additional fitting parameters to describe the feature of these multielectron edges. The k^2-weighted $\chi(k)$ plot in Figure 1 shows the prominent $KM_{4,5}$ and $KM_{2,3}$ multielectron excitation features at 10.3 and 12.7 Å^{-1} that are effectively removed using the above procedure. This increases the useable portion of the k data to about 13 Å^{-1}. For the L_2-edge spectra in Figure 1, there are weak edgelike features at about 1.5 and 4.1 Å^{-1} that are tentatively assigned to the $KN_{4,5}$ and $KN_{2,3}$ multielectron transitions. These do not significantly distort the high-frequency, multiple scattering signal at the L_2-edge that is used to evaluate the first-shell coordination structure.

2.3. XAFS Modeling. We acquired XAFS spectra at all three L-edges, although the L_2-edge data were the most useful for this analysis. The energy ranges between the L_3- and L_2-edges and the L_2- and L_1-edges are 173 and 282 eV, corresponding to k ranges of 6.7 and 8.6 Å^{-1}, respectively. The longer k range available for the L_2-edge is the most favorable for XAFS analysis, although this signal can be degraded since the XAFS signal from L_3-edge can extend into the region above the L_2-edge.[13] In the case of hydrated ions, this interference is not significant because (i) at $k > 6\ \text{Å}^{-1}$ the XAFS signal is dominated by only single scattering events, (ii) in aqueous systems there

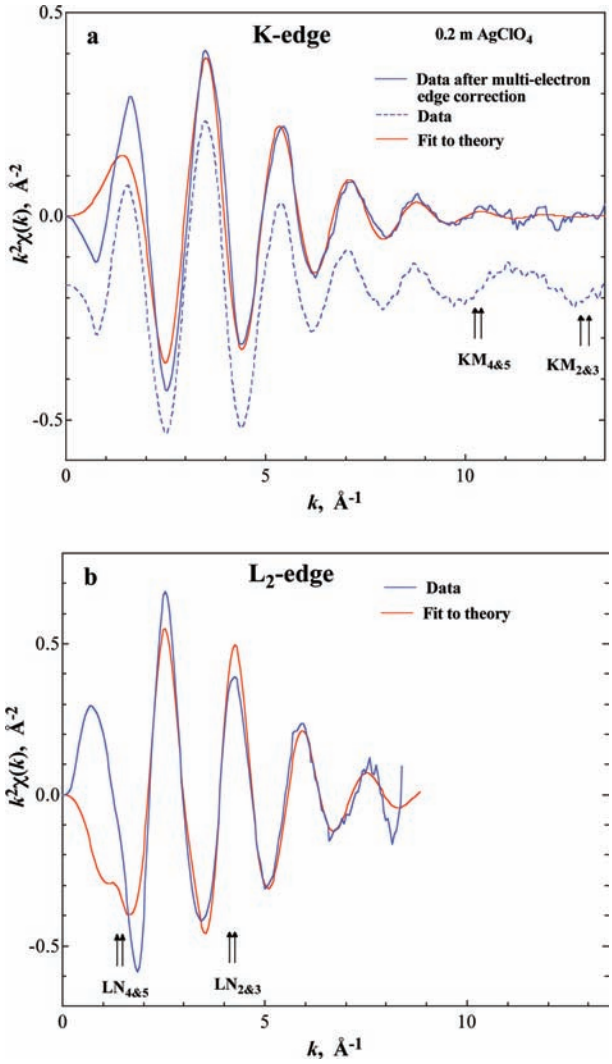

Figure 1. (a) Ag K-edge, k^2-weighted $\chi(k)$ plots for 0.2 *m* $AgClO_4$ solution. The fitted lines (red) are results from the FEFF8 standard and parameters listed in Table 2 for the trigonal bipyramidal model. The solid blue line is after removal of the multielectron excitations at $k = 10.5$ and 13 $Å^{-1}$ (see the Supporting Information). (b) Ag L_2-edge, k^2-weighted $\chi(k)$ plots.

is no signal from second and higher solvation shells, (iii) and the single scattering signal from L_3-edge that extends into the L_2-edge will have a frequency that is far below that of L_2-edge Ag−O scattering (from the energy- to momentum-transform relationship, $k = (2m_e(E - E_0)/\hbar^2)^{1/2}$. Any of the residual L_3 single scattering signal would appear in the L_2 $|\tilde{\chi}(R)|$ data at a distance equivalent to about one-quarter of the Ag−O distance. This means that residual L_3 signal will be efficiently removed with the background function. We found that the L_3- and L_2-edge $|\tilde{\chi}(R)|$ spectra are nearly identical in all respects (see the Supporting Information) including the locations and amplitudes of the Ag−O single and multiple scattering features at 1.8 and 3.5 Å, respectively. The L_1-edge spectrum was considerably noisier than the other L-edge spectra, since the cross section is significantly lower. However, within the limits of the experimental noise, the L_1- and K-edge spectra are identical including the location and amplitude of the multiple-scattering feature at 3.5 Å (see the Supporting Information).

The K-edge spectrum has the longest available *k* range (to $k = 13$ $Å^{-1}$), thus providing the best opportunity to resolve the Ag−O bond distance and bond disorder, whereas the first-shell symmetry information is contained within the multiple scattering features of both the K- and L_2-edge spectra. There are primarily five different multiple scattering paths that contribute to the measured signal to varying degrees. These are (i) O−Ag−O collinear paths with three legs, (ii) O−Ag−O collinear paths with four legs, (iii) Ag−O double return paths, (iv) O−Ag−O paths with a 90° return through Ag, and (v) Ag−O−O triangular path with a 135° leg. Unless otherwise noted, the distances of the first four multiple scattering paths were constrained to 2 times the Ag−O distance. For the double return and the 90° paths, the Debye−Waller factor was set at 4 times σ^2 of the single scattering Ag−O path. The existence of Ag−H single scattering paths was tested, but inclusion of these paths had no effect on the quality of the fits.

2.4. XAFS Spectra from Molecular Dynamics Simulations. Using both accurate energetics to describe the interactions among H_2O and Ag^+ and complete sampling of the Ag^+ solvation configuration space under the appropriate conditions should provide an accurate measure of the oxygen coordination number and symmetry around Ag^+. Here we compare two characteristic descriptions that are commonly used to obtain molecular interaction energies: (1) Coulomb plus Lennard-Jones and (2) density functional theory. The interaction expressed by description 1 was chosen because of computational convenience and as a simple test of an electrostatic treatment using point charges to compare with a fuller description (2) that explicitly treats the electronic structure of the Ag^+, the solvent water molecules, and the coupling between them. We note that DFT is not the most accurate representation of the electronic structure when compared with better ab initio methods that include a more explicit treatment of electron correlation such as MP2 and CCSD(T). Moreover, describing the dynamics classically, compared to using quantum statistical mechanics (zero-point effects), neglects other effects that may subtly influence the quantification of the oxygen coordination and symmetry about the Ag^+ ion. But, doing a full condensed-phase quantum statistical mechanical simulation at the CCSD(T) level is not feasible, even on the largest supercomputers. Both MM[30] and QM/MM[12] approaches have been performed for Ag^+ in water; however, both have Ag−O distances (MM = 2.3 Å and QM/MM = 2.6 Å) that are inconsistent with experiment (2.4 Å, the maximum in the pair distribution function peak from the MD-XAFS that best matches the experiment). Moreover, a consistent treatment of the interface between the QM and MM regions is still needed. Thus, the DFT description is used to try and capture the electronic delocalization and transfer effects known to occur in these aqueous systems. This choice is better than a simple Coulomb description but not as complete as CCSD(T). Since we are trying to describe liquid water with an Ag^+ ion, it is important to recognize that a given DFT functional treated classically may not describe certain observables. In the case of the PBE DFT functional used in the present study, it has been shown that it has a melting temperature near 417 K.[31] The best DFT description of liquid water is still an outstanding issue in the condensed-phase chemical physics community.[32,33]

Given these caveats, MD-XAFS is a powerful method to test the quality of the simulated structure against the experimental value.[21,34,20] It provides a rigorous test of bond distances, disorder, first shell symmetry, and, to a lesser extent, the coordination number. The method exactly treats all aspects of the secondary structure such as the angular correlations between first-shell water molecules that give rise to multiple scattering as well as the treatment of the long-range tail of the first peak in the Ag−O pair distribution that is often only treated by semiempirical techniques. Conversely, the simulated structure

can often be used to understand how various structural details within the experimental system contribute to the overall scattering signal. In the MD-XAFS method, an individual snapshot from an MD simulation is selected and the coordinates of all the oxygen atoms within 10 Å of a Ag^+ ion are used as input to calculate its XAFS spectra using the FEFF8 ab initio scattering code. This procedure is repeated several thousand times from a set of snapshots downloaded from the simulation. The resultant spectra are averaged to create the ensemble average spectra representing a exact description of the MD solution structure. Recently, this method was used for evaluation of the hydration structure of Ca^{2+}, K^+, and Cl^-.[20,19] The time scale of the XAFS scattering process is much shorter (<femtosecond) than the ligand exchange time scale (picosecond). Hence, XAFS probes the same average Ag−O structure that is represented by the short-range portion of the simulated pair distribution function. The pair distribution function includes the structural contributions occurring during the species interconversion (although a relatively minor component) as well as the contributions from more persistent coordination species.

We explored the hydration structure about Ag^+ using molecular dynamics simulations employing both DFT-based description of the intermolecular interactions as well as classical potentials of the Lennard-Jones plus Coulomb type. Both DFT and classical interactions were used in molecular dynamics simulations employing the CP2K ab initio molecular dynamics software package.[35] The DFT interactions were used to describe the Ag^+ and 64 H_2O system in a cubic box of volume 12.42 × 12.42 × 12.42 $Å^3$. The system size was chosen to include both the first and second solvation shells and was confirmed by inspection of the radial distribution functions. In the present study, we employ the PBE functional with a DZVP-MOLOPT-SR-GTH and GTH-PBE basis set and pseudopotential, respectively. The DFT-MD simulations using the PBE functional where carried out at 400 K, since PBE water behaves as a supercooled liquid at ambient conditions[36] with a time step of 0.5 fs for a total of 40 ps from which 1100 equally spaced configurations were chosen for XAFS analysis. This higher temperature partially remedies deficiencies in the DFT description of the interactions and should have only a minor effect of the first-shell hydration structure, since the Ag^+/water binding energies are quite high. The classical potential employs the SPC/E rigid-body water model to describe the water−water interactions. The classical potential was used on the Ag^+ and 216 H_2O system in a cubic box of volume 18.63 × 18.63 × 18.63 $Å^3$. For the classical interactions simulation, the time step was 2.5 fs and was run for a total of 10 ps from which 200 equally spaced configurations were chosen for XAFS analysis. The classical interaction runs were shorter than the corresponding DFT runs, as they converged toward equilibrium much more rapidly and showed fewer fluctuations once reaching equilibrium than the DFT runs. It appears that, in the DFT runs, several metastable states exist that the system fluctuates between at equilibrium. Future work will address these issues in greater detail. For the Ag^+/water interaction we use a Lennard-Jones plus Coulomb interactions. To better understand the sensitivity of the XAFS spectra on the Ag−O distance, we used two different repulsive wall parameters: $\sigma_{LJ} = 2.75$ Å and 2.98 Å. The LJ well-depth parameter was the same for both cases, $\varepsilon = 61.33$ K, and the Ag charge was set to $q = +1.0$ e for the Coulomb interactions.

3. Results and Discussion

3.1. K-Edge Multiple Scattering Features. Multiple scattering features in the K- (or L_2-) edge spectra for aqueous Ag^+ have not been reported in previous XAFS studies. We thus start by comparing the characteristics of these features to those of a hydrated divalent ion (Ni^{2+}) that is known to contain a significant multiple scattering feature. In the XAFS scattering process, a core electron that is ejected from the Ag atom is scattered by nearby O atoms. The most significant scattering process is single backscattering, whereby this photoelectron is scattered by an oxygen atom on a nearby water. There are also significant contributions from a process wherein the photoelectron is scattered by more than one atom. It is well-known that these multiple scattering features provide additional information about the coordination symmetry that is not available from just the single scattering data. The multiple scattering process gives rise to features in the radial structure plots, $|\tilde{\chi}(R)|$, that appear at a distance that is approximately 2 times the metal−water single scattering distance. A multiple scattering feature in the Ag K-edge spectra is shown in the k^2-weighted $|\tilde{\chi}(R)|$ spectra given in Figure 2 in the region around 3.5 Å. For comparison to the Ag^+ spectra, the spectra of Ni^{2+} and K^+ are also shown. The hydration structure about Ni^{2+} represents a well-ordered octahedral structure with exactly six H_2O's at a distance of about 2.05 Å. The collinear O−Ni^{2+}−O scattering paths are known to give rise to a relatively strong multiple scattering feature at about 3.1 Å (see Figure 2). The Ni multiple scattering feature has somewhat higher amplitude and a slightly shorter distance than the Ag feature. The prominence of the Ag multiple scattering feature was unexpected since Ni^{2+} has a highly ordered hydration shell as a result of it being a divalent ion and with a much shorter metal−water distance of 2.05 Å versus approximately 2.35 Å for the monovalent Ag^+. The presence of an Ag multiple scattering feature implies that the Ag hydration shell is relatively well ordered with a dominant symmetry. This suggests that the water might have site-specific bonding to mixed valence orbitals on the Ag^+. For further comparison, Figure 2 also shows XAFS results[19,20] for the hydrated K^+ ion that has a disordered arrangement of approximately six H_2O's at a distance of about 2.73 Å. In this case there is little or no multiple scattering feature.

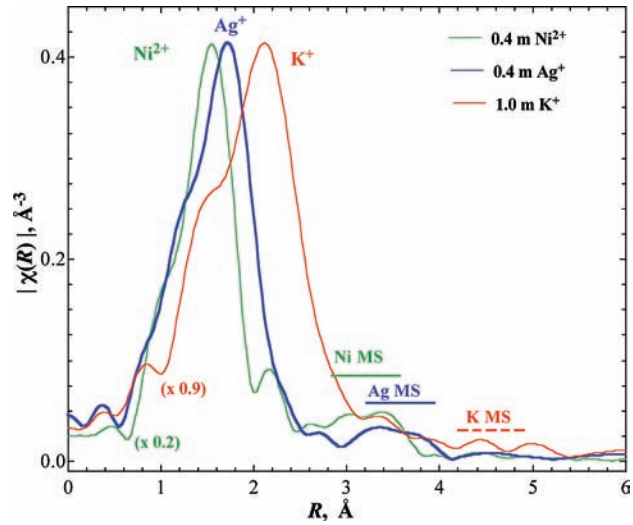

Figure 2. Comparison of the K-edge, k^2-weighted $|\tilde{\chi}(R)|$ for hydrated Ni^{2+}, Ag^+, and K^+. The amplitudes of the Ni and K spectra are scaled by factors of 0.2 and 0.9, respectively.

The Ag^+ multiple scattering feature is unchanging over a concentration range from 0.06 to 0.2 *m* Ag^+ (see Supporting Information) showing that there is no contribution from ion pairing at these concentrations. The inverse transform, $\chi(q)$, of the multiple feature at 3.5 Å shows high-frequency oscillations

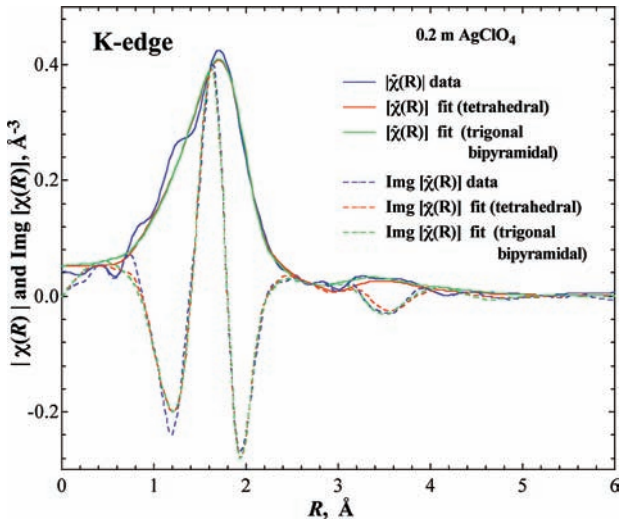

Figure 3. Fitting the K-edge spectra using tetrahedral and trigonal bipyramidal models. The silver K-edge, k^2-weighted $|\tilde{\chi}(R)|$ and Im $[\tilde{\chi}(R)]$ plots are represented for aqueous 0.2 *m* $AgClO_4$. The experimental data and the two-model fit are shown. The fitted lines are results from the FEFF8 standard and parameters listed in Table 1.

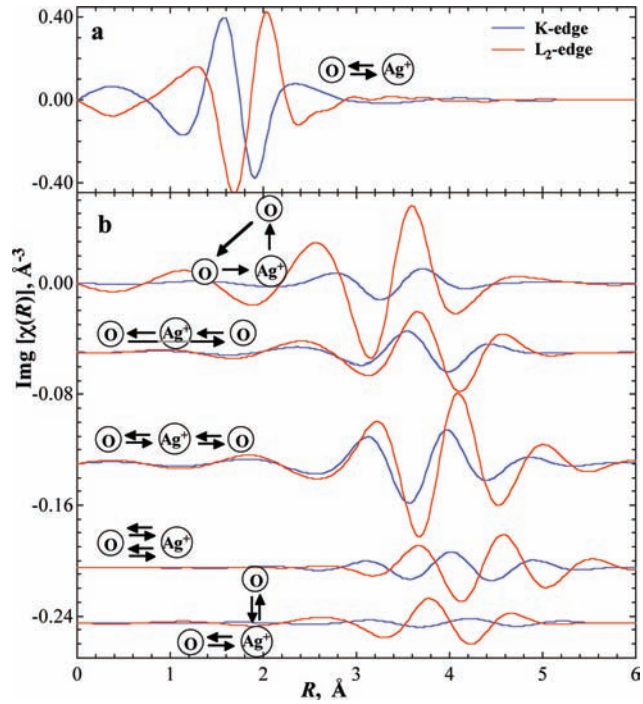

Figure 4. Comparison of various Im $[\tilde{\chi}(R)]$ scattering spectra generated from FEFF8 for aqueous Ag^+. (a) The single scattering path and (b) various multiple scattering paths corresponding to most of the scattering paths that are part of a trigonal bipyramidal structure. In all cases scattering parameters were set to the following values: $\sigma_{MS}^2 = 0.075$ Å^2 and $E_0 = 0$ eV. Various plots for the multiple scattering paths are offset for clarity.

in the range from 2 Å^{-1} < k < 6 Å^{-1} (in both K- and L_2-edge spectra; see the Supporting Information). In addition, changes in the k-range of the Fourier transform from 2−11 to 3−11 Å^{-1} had little effect on this feature. The multiple scattering features in the K-edge $|\tilde{\chi}(R)|$ plot are mirrored in L_2-edge $|\tilde{\chi}(R)|$ plot (see Figure 6). The L_2-edge multiple scattering feature has much larger amplitude in comparison to the K-edge primarily, because the core hole lifetime broadening at the K-edge is significantly higher than at L_2-edge (lifetime broadening is 6.75, 4.88, 2.57, and 2.40 eV for the K-, L_1-, L_2-, and L_3-edges, respectively).[16,25,37]

3.2. Fitting K-Edge Spectrum to Structural Models. We start by initially evaluating only the K-edge spectrum in order to demonstrate the limited ability to resolve the first-shell symmetry. We selected both four- and five-coordinate models represented by tetrahedral and trigonal bipyramidal symmetries. The tetrahedral model was selected upon the basis of the commonly accepted hydration structure of Ag^+, whereas the trigonal bipyramidal model more closely mimics the symmetry of simulated gas-phase clusters. Figure 3, compares the k^2-weighted $|\tilde{\chi}(R)|$ and Im $[\tilde{\chi}(R)]$ plots for these two models to the experimental data. The structural parameters derived from these fits are tabulated in Table 1. Both models adequately reproduce the multiple scattering features at about 3.5 Å and the quality of fits is the same. A third model involving a distorted octahedral (2 + 4) symmetry was also evaluated (not shown) and it was also found to fit the multiple scattering features at 3.5 Å. Hence, it is not possible to resolve details of the first shell symmetry with only the K-edge spectra.

3.3. Symmetry-Dependent K- and L_2-Edge Multiple Scattering. The primary objective of this study is to evaluate the multiple scattering signals in the K- and L_2-spectra in order to derive structural information about the first hydration shell. The K- and L_2-edge multiple scattering spectra provide independent rather than redundant measurements of the first shell symmetry. This is illustrated in the Im $[\tilde{\chi}(R)]$ plots shown in Figure 4 in which multiple scatterings from a number of different paths are compared. Different combinations of these paths are used to model either trigonal bipyramidal or tetrahedral symmetries. These spectra were generated using FEFF8 while fixing $\sigma_{MS}^2 = 0.075$ Å^2 for all paths to a value that is approximately equivalent to experimental values. First we notice that the O−Ag−O path with a 90° return (lowest plot in Figure 4b) contributes significantly to the L_2-edge but this path contributes negligibly to the K-edge. As pointed out by Kuzmin[13] for the symmetry of this path, the scattering is only weakly allowed at the K- or L_1-edge (s-electron initial state) but fully allowed for the L_2- or L_3-edges (2p-electron initial state). For similar reasons, the Ag−O−O triangular scattering path shown in Figure 4b also has much higher amplitude for the L_2- or L_3-edges. The other significant characteristics in Figure 4b is a comparison of the O−Ag−O collinear paths having three and four legs and the Ag−O double return paths. These are the primary scattering paths that allow one to differentiate a pure tetrahedral geometry from alternate structures that may contain collinear O−Ag−O. (A collinear geometry contains contribu-

TABLE 1: Fit to K-Edge XAFS of the Ag^+ First Shell Structure under Ambient Conditions for 0.2 *m* Ag^+ in Water

	structure					
model	N	R, Å	$\sigma^2 \times 10^3$, Å^2	$\sigma_T^2 \times 10^3$,[a] Å^2	$\sigma_{CL}^2 \times 10^3$,[a] Å^2	$\mathscr{R}$[b]
trigonal bipyrimidal	4.5(0.2)	2.331(011)	17.6(1.8)	19.2(30.2)	65.9(71.5)	0.038
tetrahedral	4.5(0.2)	2.330(011)	17.5(1.7)	25.4(29.1)		0.038

[a] The subscripts T and CL refer to triangular and collinear, respectively. [b] Goodness of fit defined by a scaled sum of squares as described in FEFFIT.

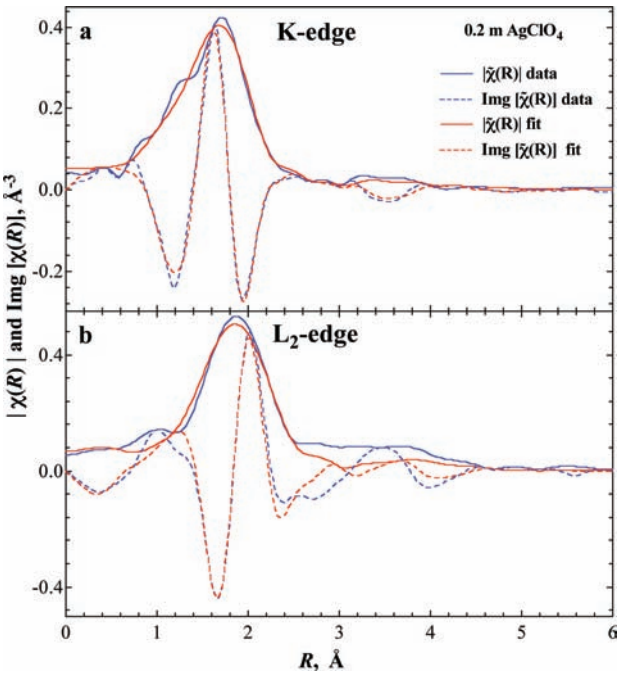

Figure 5. Fitting the K- and L_2-edge spectra using tetrahedral hydration structure. (a) Silver K-edge, k^2-weighted $|\tilde{\chi}(R)|$ and Im $[\tilde{\chi}(R)]$ plots for hydrated Ag^+ in 0.2 *m* $AgClO_4$. (b) Silver L_2-edge, k^2-weighted $|\tilde{\chi}(R)|$ and Im $[\tilde{\chi}(R)]$ plots. The experimental data and the model fit are shown. The fitted lines are results from the FEFF8 standard and parameters listed in Table 2.

tions from all three paths.) As shown in Figure 4, the three- and four-leg collinear paths are phase-shifted by approximately $\pi/2$ between the K- and L_2-edges. In contrast, the double return Ag−O path is phase-shifted by about π. It is these differences that allow one to gain an independent measure of the first shell symmetry from the L_2-edge and that provide the potential to differentiate a purely tetrahedral geometry from those structures containing collinear or 90° O−Ag−O bonds.

In Figure 4, the amplitudes of the collinear paths having three and four legs and the Ag−O double return paths differ by approximately a factor of 2 between the K- and the L_2-edge spectra. As previously described, this is primarily due the core hole lifetime broadening at the K-edge (6.75 eV) that is significantly larger than at the L_2-edge (2.40 eV). This amplitude difference is another way in which the K- and L_2-shells provide a unique measure of the first shell structure.

3.4. Fitting K- and L_2-Edge Spectra to Structural Models. The strategy is to first test existing models of Ag^+ hydration by simultaneously fitting both the K- and L_2-edge multiple scattering data and then to explore the validity of other structures that are predicted from gas-phase and liquid-phase theoretical calculations. Initially, we found that the Ag−O single scattering path from FEFF8 theoretical standards does not replicate any part of the multiple scattering features near 3.5 Å in either the K- and L_2-edge spectra (see Figure 5). Thus, multiple scattering paths from specific types of local symmetries need to be included in order to replicate these features in the spectra. Earlier scattering and XAFS studies suggested a regular tetrahedral geometry. For this geometry there are two multiple scattering paths: the Ag−O double return path and the O−Ag−O triangular scattering path. As shown in Figure 5a,b, this tetrahedral model does a reasonable job of fitting the multiple scattering feature at 3.5 Å in the K-edge spectrum but completely fails to capture the structure in the L_2-edge spectrum. At the L_2-edge, the double return scattering would undergo a π phase shift (see Figures 4 and 5), but this feature is not present in the spectrum. Hence, we can say with high confidence that the structure is not a regular tetrahedron. This confirms the supposition by Persson[9] that the structure is not a regular tetrahedron.

We next screened a series of regular symmetries such as octahedral, distorted octahedral, trigonal bipyramidal, square planar, and square pyramidal. The results point strongly to the existence of nearly collinear and 90° O−Ag−O bonds. These symmetry features provide the only scattering paths that fit the multiple scattering features in the L_2-spectrum. Gas-phase cluster calculations by Kim[1] show a tendency to form collinear O−Ag−O structures (178°) for all cluster sizes in the range of $Ag^+(H_2O)_{2-6}$. In addition, a large number of configurations show three-coordinate species in which the bond angle for two of the three water molecules is about 85°. QM/MM molecular dynamics simulations of Rode[12] for the liquid-phase Ag^+ show both 5- and 6-coordinate species with a dominant O−Ag−O bond angle at about 87° and a secondary bond angle at about 160° [although the Ag−O bond length (2.6 Å) appears to be anomalously long]. Hence, the Ag−H_2O bonding favors collinear and 90° structures, in agreement with features of the L_2-edge multiple scattering.

The parameters listed in Table 2 give the results for the corefinement of the theoretical standards to the experimental K- and L_2-edge spectra for the regular tetrahedral, trigonal bipyramidal, and distorted octahedral (2 + 4) models. A trigonal bipyramidal model satisfies the requirement for water arranged in collinear and 90° structures and also agrees with the measured coordination number of approximately 4.8 (uncertainty is ±15% from the estimate of S_0^2). The distorted octahedral model, having two waters at a short distance and four at a slightly longer distance, also captures the collinear and 90° bond angle features. This "2 + 4" model was a primary candidate from QM/MM molecular dynamics of Rode[12] and from the XAFS results of Persson.[9] As reported in Table 2, this model returns short Ag−O

TABLE 2: Global Fit to K- and L_2-Edge XAFS of the Ag^+ First Shell Structure under Ambient Conditions for 0.2 *m* Ag^+ in Water

	structure							
model	*N*	*R*, Å	$\sigma^2 \times 10^3$, Å^2	$C_3 \times 10^4$, Å^3	$\sigma_T^2 \times 10^3$,[a] Å^2	$\sigma_{CL}^2 \times 10^3$,[a] Å^2	$\sigma_{90}^2 \times 10^3$,[a] Å^2	$\mathcal{R}$[b]
trigonal bipyrimidal	4.8(0.2)	2.317(019)	15.6(1.1)	0.3(4.1)	71.6(58.4)	56.1(20.2)	32.8(40.7)	0.024
distorted octahedral	2.3(0.1) 4[c]	2.331(016) 2.507(058)	9.3(2.4) 48.3(9.6)		13.7(8.6)	20.2(15.1)	11.0(24.3)	0.019
tetrahedral	4.2(0.2)	2.349(014)	19.3(2.2)	5.8(5.6)	41.8(25.3)			0.049

[a] The subscripts T, CL, and 90 refer to triangular, collinear, and 90° double return paths, respectively. [b] Global goodness of fit for both K and L_2 data. [c] Coordination number fixed at 4 in the fitting.

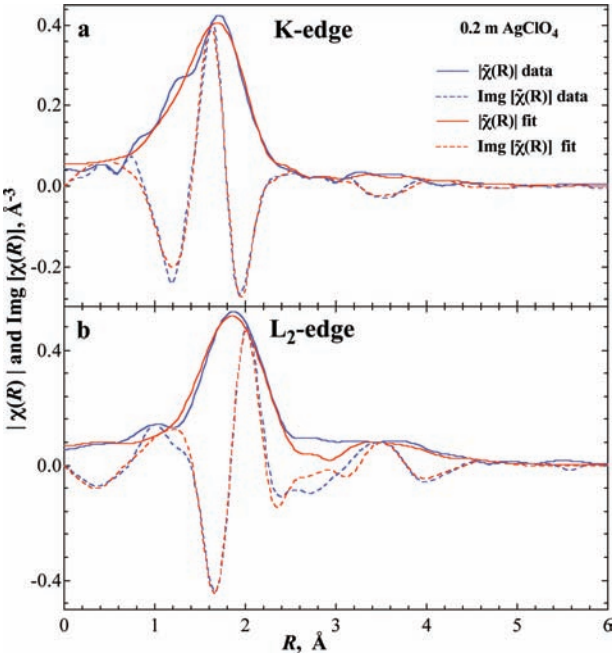

Figure 6. Fitting the K- and L_2-edge spectra using a trigonal bipyramidal hydration structure. (a) Silver K-edge, k^2-weighted $|\tilde{\chi}(R)|$ and Im $[\tilde{\chi}(R)]$ plots for hydrated Ag^+ in 0.2 *m* $AgClO_4$. (b) Silver L_2-edge, k^2-weighted $|\tilde{\chi}(R)|$ and Im $[\tilde{\chi}(R)]$ plots. The experimental data and the model fit are shown. The fitted lines are results from the FEFF8 standard and parameters listed in Table 2.

distances for two waters of 2.33 Å with four waters at a longer distance of 2.51 Å. The ability to fit the multiple scattering features of the K- and L_2-edge is nearly the same (see the Supporting Information) as that for the fit to the trigonal bipyramidal model shown in Figure 6. There is a modest improvement in the quality of fit ($\mathscr{R}$ factor) for the "2 + 4" model over the trigonal bipyramidal as reported in Table 2. In the XAFS fitting, the uncertainty in determining the coordination number for the longer-distance water shell is relatively high; thus, it is not possible to tell whether there are three or four waters in this second shell. This "2 + 4" model returns an average bond distance of 2.45 Å that is substantially shorter than the average bond length of 2.6 Å reported in the QM/MM study of Rode.[12] A coordination number of 5 or 6 for an average Ag−O bond distance of 2.45 Å is in reasonable agreement with a value of 5.4 that would be predicted from the empirical correlation between bond distance and coordination number for Ag(I) compounds given by Shannon.[38,39] None of the models completely capture all of the features of both the K- and L_2-edge spectra in Figure 6. This likely means that these standard symmetry models cannot completely describe the true fluxional structure whose time-average structure likely has significant distortions from a regular symmetry. However, as expected, both the trigonal bipyramidal and distorted octahedral models provide a large improvement in the goodness-of-fit over the tetrahedral model.

3.5. DFT-Based and Classical Molecular Dynamics Results. The Ag^+ structures from a series of different MD simulations were used to generate the XAFS spectra that are shown in Figure 7. In Figure 7a, the $\chi(k)$ plots show that the DFT-based model and the two classical Lennard-Jones (SPC/E) models do not quantitatively recover both the amplitude and frequency of the experimental $\chi(k)$ oscillations. Notably, the DFT-model accurately captures the frequency of the oscillations, although it under-represents the envelope of their amplitude, especially at low *k*. In Figure 7b,c, the $|\tilde{\chi}(R)|$ or radial structure

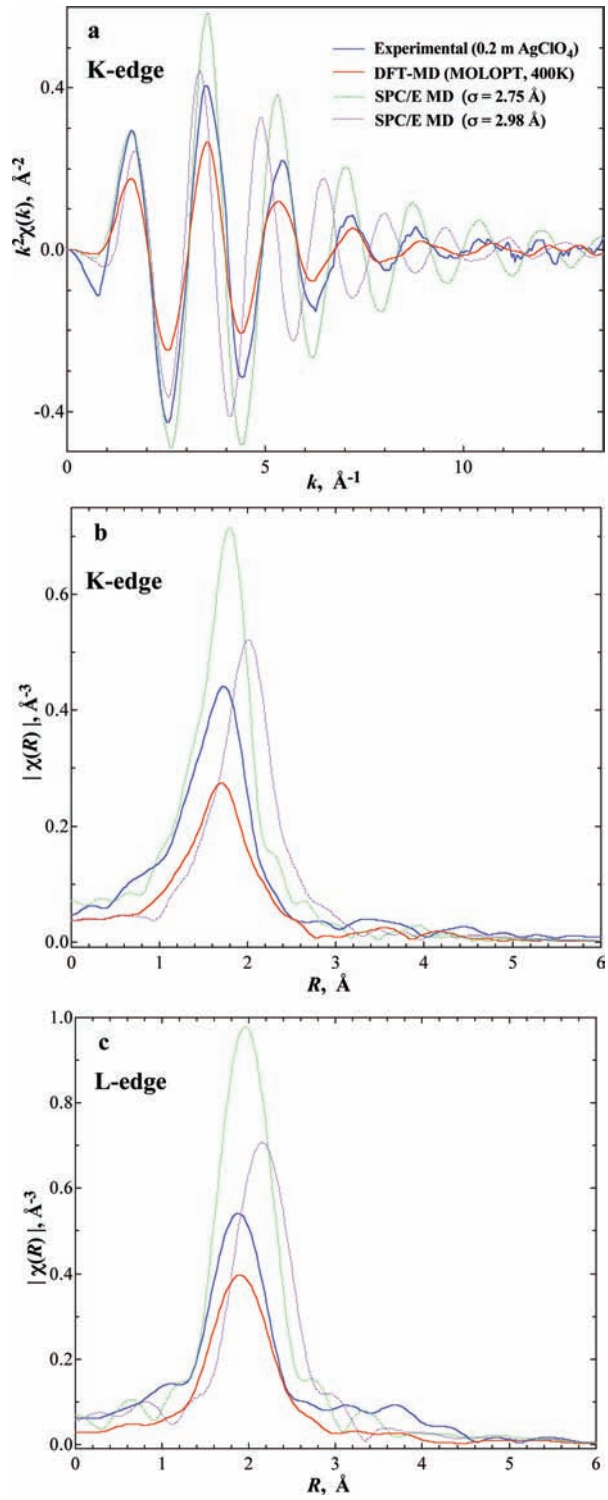

Figure 7. Comparing experimental spectra to MD-XAFS spectra generate from DFT and classical potential molecular dynamics simulations. (a) K-edge, k^2-weighted $\chi(k)$ plots, (b) K-edge, k^2-weighted $|\tilde{\chi}(R)|$ plots, (c) L_2-edge, k^2-weighted $|\tilde{\chi}(R)|$ plots.

plots for both K- and L_2-edge spectra further illustrate the differences between simulated and experimental structure. An initial SPC/E model ($\sigma_{LJ} = 2.98$ Å) generated a first-shell Ag−O peak that is located at a distance that is 0.23 Å longer than for the experimental system. A second SPC/E model, using a refined σ_{LJ} parameter ($\sigma_{LJ} = 2.75$ Å), yielded a reasonable Ag−O distance but significantly degraded the amplitude of the Ag−O peak. In Table 3 the coordination numbers *N*, the Ag−O distance peak *R*, and the variance σ^2 from the simulation are reported.

TABLE 3: Structural Parameters Characterizing the First Peak in the Ag−O Pair Distribution Function Determined from Molecular Dynamics Simulations

	structure		
model	N^a	R,[b] Å	$\sigma^2 \times 10^{3,b}$ Å^2
DFT-MD (MOLOPT)	4.2	2.44	20.1
SPC/E MD $\sigma_{LJ} = 2.75$ Å	5.7	2.42	10.1
SPC/E MD $\sigma_{LJ} = 2.98$ Å	5.9	2.62	12.8

[a] From integration of the first peak in the Ag−O pair distribution function to the first minimum. [b] From centroid and variance of Gaussian function fitted to the first peak in the Ag−O pair distribution function.

The coordination numbers were calculated via spherical integration of the radial distribution function $g(r)$. The Ag−O distance peak R and variance σ^2 in Table 3 were calculated from the centroid and variance of a Gaussian fit to the first peak in the $g(r)$ neglecting any data beyond the point of inflection. These parameters are defined in a slightly different way than those extracted from the XAFS fitting reported in Tables 1 and 2.[20]

The DFT method accurately treats electronic effects (e.g., aqueous stereochemistry, charge transfer, interatomic electric field strengths), whereas the classical potentials only partially treat these effects in an empirical way. On the other hand, the DFT method does not explicitly include the important effects of dispersion and zero-point-energies, whereas for the classical potential these effects are, in part, included in the parametrization. Overall, the roles of these energetic effects certainly influence the underlying structure and symmetry and thereby influence the resulting XAFS signal. It is significant that DFT does a better job of predicting the distance and the width of the pair distribution without adjustable parameters; however, further research is needed to better quantify these effects. Only the DFT method is capable of describing the site-specific binding of water to the valence orbitals of the Ag ion. It is not surprising then that the SPC/E models do not yield appreciable multiple scattering signals (Figure 7b,c) from symmetrically oriented water molecules in the first shell. The DFT method generates multiple scattering signals that reproduce some of the features of the experimental spectra; however, the multiple scattering amplitudes are lower than the experimental values. This suggests that the first-shell water is even more symmetrically oriented about Ag^+ than predicted by the DFT method. It seems that the treatment of the electronic effects within the DFT method is beginning to provide a more accurate description of the Ag−O distances, the symmetry, and the distribution (i.e., Debye−Waller factors) of the oxygen atoms in the first solvation shell.

Conclusions

We have corefined fits to K- and L_2-edge data to resolve the hydration structure of aqueous Ag^+. We use the method of symmetry-dependent multiple scattering analysis as a rigorous test of proposed first-shell symmetry. The conventional view of the pure tetrahedral structure does not match the multiple scattering features. A structure with nearly collinear and 90° O−Ag−O bonds matches the measured K- and L_2-edge spectra. For this second row transition metal, the site-specific bonding of water to hybridized valence orbitals of the Ag^+ plays a leading role in the hydration structure, in contrast to the structure for Na^+, wherein water interactions are more ionic and there is no local symmetry. For Ag^+, both trigonal bipyramidal and distorted octahedral (2 + 4) models match both the multiple scattering features and the fitted parameters. The K- and L_2-edge spectra can be used as a rigorous test of new generations of molecular simulations, since the experimental results impose requirements for highly specific symmetries, bond distances, and disorder. The method of symmetry-dependent multiple scattering analysis will have important applications to the studies of other aqueous ions as well as to other systems in catalysis and materials science.

Acknowledgment. This work was supported by the U.S. Department of Energy (DOE), Office of Basic Energy Sciences, Division of Chemical Sciences, Geosciences and Biosciences. PNNL is operated for the Department of Energy by Battelle. PNC/XOR facilities at the Advanced Photon Source, and research at these facilities, are supported by the U.S. Department of Energy—Basic Energy Sciences, a major facilities access grant from NSERC, the University of Washington, Simon Fraser University, the Pacific Northwest National Laboratory, and the Advanced Photon Source. Use of the Advanced Photon Source is also supported by the U.S. Department of Energy, Office of Science, Office of Basic Energy Sciences, under Contract DE-AC02-06CH11357.

Supporting Information Available: XAFS spectra and analysis. This material is available free of charge via the Internet at http://pubs.acs.org.

References and Notes

(1) Lee, E. C.; Lee, H. M.; Tarakeshwar, P.; Kim, K. S. Structures, energies, and spectra of aqua−silver(I) complexes. *J. Chem. Phys.* **2003**, *119* (15), 7725–7736.

(2) Feller, D.; Glendening, E. D.; de Jong, W. A. Structures and binding enthalpies of M+ (H_2O)(n) clusters, M=Cu, Ag, Au. *J. Chem. Phys.* **1999**, *110* (3), 1475–1491.

(3) Holland, P. M.; Castleman, A. W. The thermochemical properties of gas-phase transition-metal ion complexes. *J. Chem. Phys.* **1982**, *76* (8), 4195–4205.

(4) Yamaguchi, T.; Johansson, G.; Holmberg, B.; Maeda, M.; Ohtaki, H. The coordination and complex-formation of silver(I) in aqueous perchlorate, nitrate, and iodide solutions. *Acta Chem. Scand. Ser. A-Phys. Inorg. Chem.* **1984**, *38* (6), 437–451.

(5) Skipper, N. T.; Neilson, G. W. X-ray and neutron-diffraction studies on concentrated aqueous-solutions of sodium-nitrate and silver-nitrate. *J. Phys.: Condens. Matter* **1989**, *1* (26), 4141–4154.

(6) Sandstrom, M.; Neilson, G. W.; Johansson, G.; Yamaguchi, T. Ag^+ hydration in perchlorate solution. *J. Phys. C: Solid State Phys.* **1985**, *18* (36), 1115–1121.

(7) Yamaguchi, T.; Lindqvist, O.; Boyce, J. B.; Claeson, T. Determination of the hydration structure of silver ions in aqueous silver perchlorate and nitrate solutions from EXAFS using synchrotron radiation. *Acta Chem. Scand. Ser. A-Phys. Inorg. Chem.* **1984**, *38* (6), 423–428.

(8) Seward, T. M.; Henderson, C. M. B.; Charnock, J. M.; Dobson, B. R. An X-ray absorption (EXAFS) spectroscopic study of aquated Ag^+ in hydrothermal solutions to 350°C. *Geochim. Cosmochim. Acta* **1996**, *60*, 2273–2282.

(9) Persson, I.; Nilsson, K. B. Coordination chemistry of the solvated silver(I) ion in the oxygen donor solvents water, dimethyl sulfoxide, and N,N′-dimethylpropyleneurea. *Inorg. Chem.* **2006**, *45* (18), 7428–7434.

(10) Blumberger, J.; Bernasconi, L.; Tavernelli, I.; Vuilleumier, R.; Sprik, M. Electronic structure and solvation of copper and silver ions: A theoretical picture of a model aqueous redox reaction. *J. Am. Chem. Soc.* **2004**, *126* (12), 3928–3938.

(11) Vuilleumier, R.; Sprik, M. Electronic properties of hard and soft ions in solution: Aqueous Na^+ and Ag^+ compared. *J. Chem. Phys.* **2001**, *115* (8), 3454–3468.

(12) Armunanto, R.; Schwenk, C. F.; Rode, B. M. Structure and dynamics of hydrated Ag (I): Ab initio quantum mechanical-molecular mechanical molecular dynamics simulation. *J. Phys. Chem. A* **2003**, *107* (17), 3132–3138.

(13) Kuzmin, A.; Purans, J.; Benfatto, M.; Natoli, C. R. X-ray-absorption study of rhenium L3 and L1 edges in ReO_3—Multiple-scattering approach. *Phys. Rev. B* **1993**, *47* (5), 2480–2486.

(14) Kuzmin, A.; Purans, J. A new fast spherical approximation for calculation of multiple-scattering contributions in X-ray absorption fine-structure and its application to ReO_3, $NaWO_3$ and MoO_3. *J. Phys.: Condens. Matter* **1993**, *5* (3), 267–282.

(15) DiCicco, A. Multiple-edge EXAFS refinement: Short-range structure in liquid and crystalline Sn. *Phys. Rev. B* **1996**, *53* (10), 6174–6185.

(16) Fuggle, J. C.; Inglesfield, J. E. *Unoccupied Electonic States*; Springer-Verlag: New York, 1992; p 347−351.

(17) D'Angelo, P.; Panfilis, S.; Filipponi, A.; Persson, I. High-energy X-ray absorption spectroscopy: A new tool for structural investigations of lanthanoids and third-row transition elements. *Chem.—Eur. J.* **2008**, *14* (10), 3045–3055.

(18) Fulton, J. L.; Heald, S. M.; Badyal, Y. S.; Simonson, J. M. Understanding the effects of concentration on the solvation structure of Ca^{2+} in aqueous solution. I: The perspective on local structure from EXAFS and XANES. *J. Phys. Chem. A* **2003**, *107* (23), 4688–4696.

(19) Glezakou, V.-A.; Chen, Y. S.; Fulton, J. L.; Schenter, G. K.; Dang, L. X. Electronic structure, statistical mechanical simulations and EXAFS spectroscopy of aqueous potassium. *Theor. Chem. Acc.* **2006**, *115*, 86−99.

(20) Dang, L. X.; Schenter, G. K.; Glezakou, V. A.; Fulton, J. L. Molecular simulation analysis and X-ray absorption measurement of Ca^{2+}, K^+, and Cl^- ions in solution. *J. Phys. Chem. B* **2006**, *110* (47), 23644–23654.

(21) Palmer, B. J.; Pfund, D. M.; Fulton, J. L. Direct modeling of EXAFS spectra from molecular dynamics simulations. *J. Phys. Chem.* **1996**, *100* (32), 13393–13398.

(22) Chang, T. C. G.; Irish, D. Ion-pair formation in aqueous solutions of silver nitrate: A Raman and infrared spectral study. *J. Solution Chem.* **1974**, *3* (3), 175–189.

(23) Baes, C. F.; Mesmer, R. E., *The Hydrolysis of Cations*; Krieger Publishing Co.: Malabar, FL, 1976.

(24) Fulton, J. L.; Linehan, J. C.; Autrey, T.; Balasubramanian, M.; Chen, Y.; Szymczak, N. K. When is a nanoparticle a cluster? An operando EXAFS study of amine borane dehydrocoupling by Rh4−6 clusters. *J. Am. Chem. Soc.* **2007**, *129* (39), 11936–11949.

(25) Chen, M. H.; Crasemann, B.; Mark, H. Relativistic K-shell Auger rates, level widths, and fluorescence yields. *Phys. Rev. A* **1980**, *21* (2), 436–441.

(26) Newville, M. IFEFFIT: interactive XAFS analysis and FEFF fitting. *J. Synchrotr. Radiat.* **2001**, *8*, 322–324.

(27) Ravel, B.; Newville, M. ATHENA, ARTEMIS, HEPHAESTUS: Data analysis for X-ray absorption spectroscopy using IFEFFIT. *J. Synchrotr. Radiat.* **2005**, *12*, 537–541.

(28) Zabinsky, S. I.; Rehr, J. J.; Ankudinov, A.; Albers, R. C.; Eller, M. J. Multiple-scattering calculations of x-ray-absorption spectra. *Phys. Rev. B.* **1995**, *52*, 2995–3009.

(29) Rehr, J. J.; Albers, R. C. Theoretical approaches to X-ray absorption fine structure. *Rev. Mod. Phys.* **2000**, *72* (3), 621–654.

(30) Dubois, V.; Archirel, P.; Boutin, A. Monte Carlo simulations of Ag^+ and Ag in aqueous solution. Redox potential of the Ag^+/Ag couple. *J. Phys. Chem. B* **2001**, *105* (38), 9363–9369.

(31) Yoo, S.; Zeng, X. C.; Xantheas, S. S. On the phase diagram of water with density functional theory potentials: The melting temperature of ice I-h with the Perdew−Burke−Ernzerhof and Becke−Lee−Yang−Parr functionals. *J. Chem. Phys.* **2009**, (22), 130.

(32) Todorova, T.; Seitsonen, A. P.; Hutter, J.; Kuo, I. F. W.; Mundy, C. J. Molecular dynamics simulation of liquid water: Hybrid density functionals. *J. Phys. Chem. B* **2006**, *110* (8), 3685–3691.

(33) Lin, I. C.; Seitsonen, A. P.; Coutinho-Neto, M. D.; Tavernelli, I.; Rothlisberger, U. Importance of van der Waals interactions in liquid water. *J. Phys. Chem. B* **2009**, *113* (4), 1127–1131.

(34) McCarthy, M. I.; Schenter, G. K.; ChaconTaylor, M. R.; Rehr, J. J.; Brown, G. E. Prediction of extended X-ray-absorption fine-structure spectra from molecular interaction models: $Na^+(H_2O)_n$−MgO(100) interface. *Phys. Rev. B* **1997**, *56* (15), 9925–9936.

(35) http://cp2k.berlios.de.

(36) Kuo, I. F. W.; Mundy, C. J.; McGrath, M. J.; Siepmann, J. I. Time-dependent properties of liquid water: A comparison of Car−Parrinello and Born−Oppenheimer molecular dynamics simulations. *J. Chem. Theory Comput.* **2006**, *2* (5), 1274–1281.

(37) Sipr, O.; Rocca, F.; Dalba, G. Real-space multiple-scattering analysis of Ag L_1- and L_3-edge XANES spectra of Ag_2O. *J. Synchrotr. Radiat.* **1999**, *6*, 770–772.

(38) Shannon, R. D. Revised effective ionic-radii and systematic studies of interatomic distances in halides and chalcogenides. *Acta Crystallogr., Sect. A* **1976**, *32* (SEP1), 751–767.

(39) Beattie, J. K.; Best, S. P.; Skelton, B. W.; White, A. H. Structural studies on the cesium alums, $CsM^{III}[SO_4]_2 \cdot H_2O$. *J. Chem. Soc.-Dalton Trans.* **1981**, (10), 2105–2111.

JP9064906